12

Neuropathy Target Esterase Biosensor

Devesh Srivastava[1], Neeraj Kohli[1], Rudy J. Richardson[2],
Robert M. Worden[1], and Ilsoon Lee[1]
[1]*Department of Chemical Engineering and Materials Science, School of Engineering, Michigan State University,*
[2]*Toxicology Program, Department of Environmental Health Sciences, University of Michigan*
United States of America

1. Introduction

Neuropathy Target Esterase (NTE), is a membrane-bound protein found in neurons of vertebrates (Glynn, 1999; Atkins & Glynn, 2000; van Tienhoven et al., 2002; Li et al., 2003; Makhaeva et al., 2003; Kropp et al., 2004), has been shown to be necessary for embryonic development in mice, and is believed to be involved in cell-signaling pathways and lipid trafficking (Glynn, 1999).

NTE has serine esterase activity and can hydrolyze ester, peptide, and amide bonds. The nucleophilic serine residue (active site) of NTE attacks the carbonyl carbon atom of the substrate, forming a covalent acyl-enzyme intermediate, which is subsequently hydrolyzed. A consequence of this reaction mechanism is that the esterase activity of NTE is susceptible to covalent inhibition by organophosphorus esters (OPs) with which it forms an analogous phosphyl-enzyme intermediate.

Irreversible binding of some OP compounds to the active serine site results in a debilitating neural disease known as OP-induced delayed neuropathy (OPIDN) (Glynn, 1999). Signs of OPIDN include flaccid paralysis of the lower limbs, which becomes evident two to three weeks after exposure to neuropathic OPs. Recovery from this disease is usually poor, and there is no specific treatment. In addition, mutations in the NTE gene have been linked to motor neuron disease (Rainier et al., 2008).

Because NTE plays a central role in both chemically induced and spontaneously occurring neurological diseases, approaches that can help measure its esterase activity and inhibition are of tremendous scientific and commercial importance. Because NTE is difficult to produce for research purposes, research to study its esterase activity is typically done using a fragment of the NTE protein that contains the esterase activity and can be more easily produced. One such fragment, known as NEST, (Atkins & Glynn, 2000; Forshaw et al., 2001; Kropp et al., 2004) reacts with esters and inhibitors in a manner very similar to NTE.

Conventionally, the esterase activity of NTE (or NEST) is measured using two distinct steps. In the first step, a solution containing phenyl valerate is brought into contact with NEST or NTE protein solution, whose esterase activity reacts with a portion of the artificial substrate phenyl valerate to form phenol. In the second step, the concentration of phenol in the solution is determined either colorimetrically, in the presence of 4-amino antipyrine

Source: Intelligent and Biosensors, Book edited by: Vernon S. Somerset,
ISBN 978-953-7619-58-9, pp. 386, January 2010, INTECH, Croatia, downloaded from SCIYO.COM

(Kayyali et al., 1991), or electrochemically, in the presence of tyrosinase enzyme (Sigolaeva et al., 2001; Sokolovskaya et al., 2005). Tyrosinase converts phenol first to catechol and then to *o*-quinone, which can be measured electrochemically at an electrode (Makhaeva et al., 2003). The current generated by the electrode increases with the amount of *o*-quinone present, thus giving an indirect measurement of the amount of NTE esterase activity present during the first step. To test for esterase inhibition, this procedure is repeated both in the absence and presence of a putative inhibitor (e.g., an OP compound). A reduced signal indicates inhibition of the esterase activity. This method has the disadvantages of being slow, and requiring two steps, making it unsuitable for some important applications, such as high-throughput screening of compounds for NTE inhibition and continuous, on-line, environmental monitoring to detect chemical warfare agents that target NTE (Richardson et al., 2009). The present chapter reviews and extends our work on the first continuous, electrochemical biosensor for real-time, rapid measurement of NEST (or NTE) esterase activity. The biosensor was fabricated by co-immobilizing NEST protein and tyrosinase enzyme on an electrode using the layer by layer assembly approach by Decher (Decher, 1997). To our knowledge, this is the first time NEST has been immobilized in an active conformation on an electrode. Potential applications of this sensor include detecting the presence of chemical weapons that target NTE, screening industrial and agricultural OP compounds for NTE inhibition, studying the fundamental reaction kinetics of NTE, and investigating the effect of NTE mutations found in motor neuron disease patients on NTE's enzymatic properties. The same approach can be used for activitiy measurements of other serine hydrolases, such as acetylcholinesterase (AChE) and butyrylcholinesterase (BChE) (Kohli et al., 2007).

2. Experimental section

Materials

Thioctic acid, poly-L-lysine (PLL) (molecular weight ~ 15,000), tyrosinase (Tyr), sodium phosphate (monobasic and dibasic), ethylenediaminetetraacetic acid (EDTA), sodium chloride, 3-[(3-cholamidopropyl) dimethylammonio]-1-propanesulfonate (CHAPS) and isopropyl thiogalactoside (IPTG) were obtained from Sigma (St. Louis, MO). Ultrapure water (18.2MΩ) was supplied by a Nanopure-UV four-stage purifier (Barnstead International, Dubuque, IA); the purifier was equipped with a UV source and a final 0.2 μm filter.

NEST expression and purification

NEST was expressed and purified according to published procedures (Atkins & Glynn, 2000). Briefly, a DNA fragment encoding NEST was cloned into pET-21b vector, and the resulting expression vector was transformed into *E. coli* BL21 (DE3). An overnight culture of transformed *E. coli* was inoculated with M9 media containing ampicillin and grown in a fermentor. IPTG was added to the resulting cell culture after a day to induce the expression of NEST. The resulting cells were collected 4 h after induction by centrifugation and subjected to protein expression techniques. Briefly, 5 g of cell paste was suspended in 30 ml of PEN buffer (50mM sodium phosphate/0.3 M NaCl/0.5 mM EDTA, pH 7.8) containing 2% (w/v) CHAPS and tip sonicated four times. The cell lysate was centrifuged at 2000*g* for 30 min at 4°C, the supernatant was collected, and about 7 mL of supernatant was added to a mini column (volume 10 mL) containing 3 mL of Ni-nitrilotriacetic acid (NTA) resin. The

mini column was rotated at room temperature for 20 min, centrifuged at 2000*g* for 20 sec and then the top solution was drawn off. The histidine-tagged NEST was eluted from the Ni-NTA resin using 10 mL of PEN buffer containing 0.3% (w/v) CHAPS and 0.3 M imidazole. The protein purity was determined using SDS-PAGE and protein concentration was determined using BioRad Dc protein assay kit. For long term storage, 25% (v/v) glycerol was added to the protein solution, which was then stored at -20°C.

Preparation of gold electrode for NEST biosensor

Tyrosinase is a copper-containing oxidase (Forzani et al., 2000; Coche-Guerente et al., 2001), which possesses two different activities, as illustrated in reaction 1.

$$\textbf{phenol} \rightarrow \textbf{catechol} \rightarrow \textit{o}\textbf{-quinone} + \mathbf{H_2O} \quad (1)$$

The first step is referred to as the enzyme's hydroxylase activity (also known as cresolase activity) where phenol is hydroxylated by the aid of molecular oxygen to produce catechol. In the second step, known as the catecholase activity, the enzyme oxidizes catechol to o-quinone and is simultaneously oxidized by oxygen to its original form, with the production of water. The reaction product, o-quinone, is electrochemically active and can be reduced back to the catechol form at low applied potentials, as illustrated in reaction 2.

$$\textit{o}\textbf{-quinone} + 2\mathbf{H^+} + 2\mathbf{e^-} \rightarrow \textbf{catechol} \quad (2)$$

We exploited these characteristics of tyrosinase to fabricate a NEST biosensor, capable of measuring the NEST's esterase activity and its inhibition, by co-immobilizing NEST and tyrosinase on a gold electrode using the layer by layer assembly approach.

The molecular architecture of the biosensor interfaces are shown schematically in Figure 1 (a) & (b). Two molecular self-assembly approaches, (a) layer-by-layer (LBL) assembly (Decher, 1997) and (b) tethered lipid bilayer membranes (tBLM) (Kohli et al., 2006), were utilized in constructing nanostructured NEST biosensors. Gold electrodes cleaned in piranha solution were dipped in a 5 mM solution of thioctic acid in ethanol for 30 min. The electrodes were washed with ethanol, dried under nitrogen and dipped in PLL solution for 45 min. The PLL solution was prepared by adding 12 mg of PLL in 50 mL of 20 mM phosphate buffer (pH 8.5). The electrodes were then rinsed with water and dipped in an aqueous solution of tyrosinase (Tyr) (0.2 mg/ml) for 1 h. The last two steps were repeated varying number times to create PLL-Tyr bilayers with PLL being the topmost layer. The electrodes were washed with water and dipped in a solution of NEST protein (0.1 mg/ml) in 100 mM phosphate buffer, pH (7.0) for 1 h. The electrodes were then washed with water, dried under nitrogen and dipped in phosphate buffer (0.1 M, pH 7.0) for testing.

Preparation of phenyl valerate solution

To prepare phenyl valerate solution, 15 mg of phenyl valerate was dissolved in 1 mL of dimethylformamide (DMF), and 15 mL of water containing 0.03% (w/v) Triton-X100 was added slowly under vigorous stirring. For potential step voltammetry experiments, small aliquots of the resulting phenyl valerate micellar solution (5.286 mM nominal concentration) were added to the phosphate buffer to obtain the desired apparent concentrations.

Ellipsometry

Ellipsometric measurements were obtained with a rotating analyzer ellipsometer (model M-44; J.A. Woollan Co. Inc., Lincoln, NE) using WVASE32 software. The thickness values for

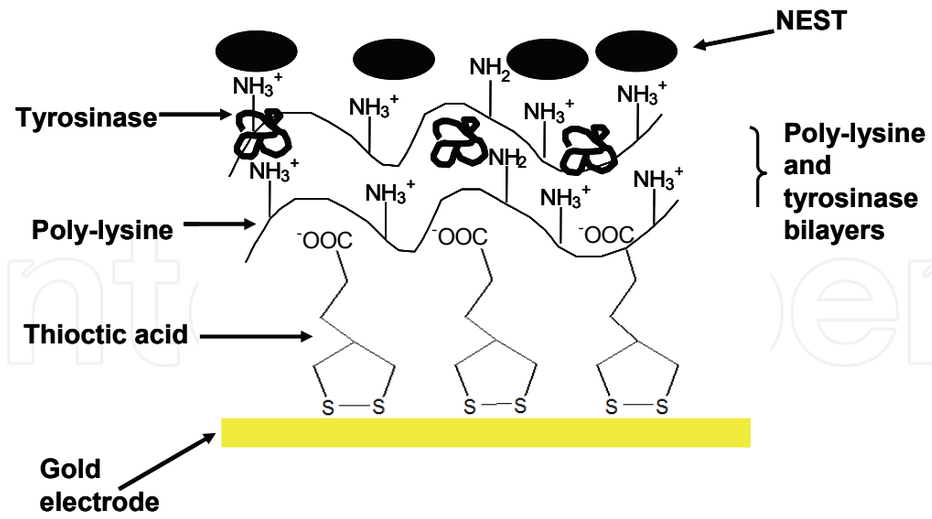

(a)

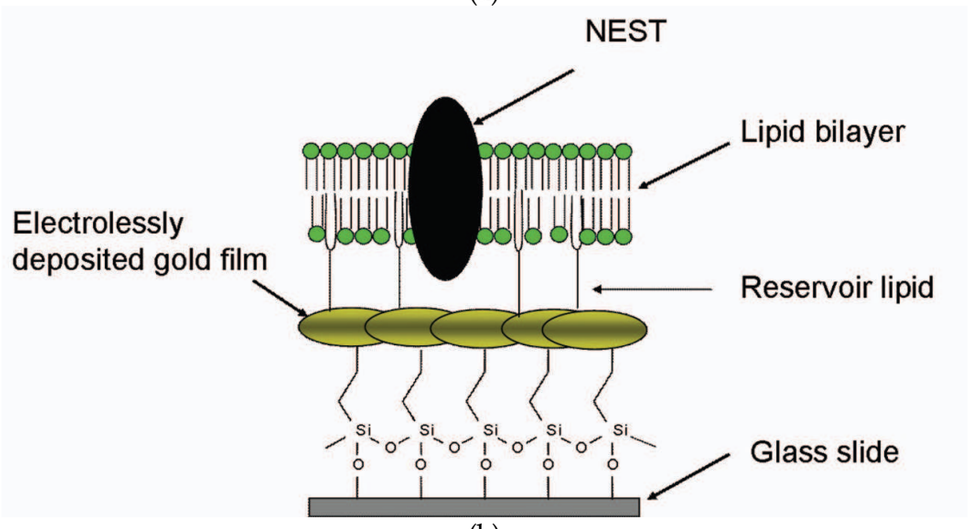

(b)

Fig. 1. Molecular architecture of the nanostructured NEST biosensors via (a) layer-by-layer (LBL) deposition scheme as adapted/reproduced with permission from (Kohli et al., 2007; Srivastava, 2008), and (b) tethered lipid bilayer membranes (tBLM) adapted with permission from (Kohli et al., 2006).

dried films were determined using 44 wavelengths between 414.0 and 736.1 nm. The angle of incidence was 75° for all experiments. Refractive indices of films containing PLL and proteins was assumed to be n=1.5, k=0. These optical constants compare well with those determined for 4 bilayer films consisting of poly-L-lysine and tyrosinase using ellipsometry.

Potential step voltammetry and other measurements

The electrodes (sensors) were maintained at a potential of -100 mV (vs Ag/AgCl reference electrode) using a BAS CV-50W electrochemical analyzer. The esterase activity of the NEST biosensor was monitored by measuring the output current for a variety of phenyl valerate concentrations, under stirred conditions. The NEST protein converts phenyl valerate to phenol, which gets converted to *o*-quinone by tyrosinase. The *o*-quinone gets reduced at the

electrode's surface, resulting in the generation of current. The electroreduction of *o*-quinone produces catechol, which again gets converted to *o*-quinone by tyrosinase, thus amplifying the signal.
To measure inhibition of the esterase activity, a known quantity of phenyl valerate was added to the phosphate buffer (pH 7.0), under stirred conditions. After the stabilization of current, a known amount of NEST inhibitor was added, and the resulting drop in current was measured.

3. Results and discussion

We have tested both LBL assembly and tBLM methods to fabricate novel nanostructured NEST biosensors, as schemed in Figure 1 (a) & (b) (Kohli et al., 2006; Kohli et al., 2007; Srivastava, 2008). In this Chapter, we will focus on the former approach. The latter is briefly summarized as below. The phenyl valerate assay was used to confirm whether tBLMs could immobilize NEST in a functional conformation. Incubation of phenyl valerate with NEST-containing BLMs on gold resulted in the production of about 2 ± 0.19 nmol/min of phenol over an area of 1 cm^2. Incubation of phenyl valerate with NEST-DOPC liposomes in solution resulted in the production of 40 ± 1.2 nmol/min of phenol per μg of NEST protein. This result suggests the immobilization of approximately 50 ng/cm^2 of active NEST in tBLMs. To our knowledge, this is the first time NEST has been immobilized in an active conformation on a surface (Kohli et al., 2006).

3.1 Ellipsometry

Ellipsometry were used to confirm the deposition of different layers that make up the NEST biosensor. As shown in Figure 2, the thickness increase following the addition of the first

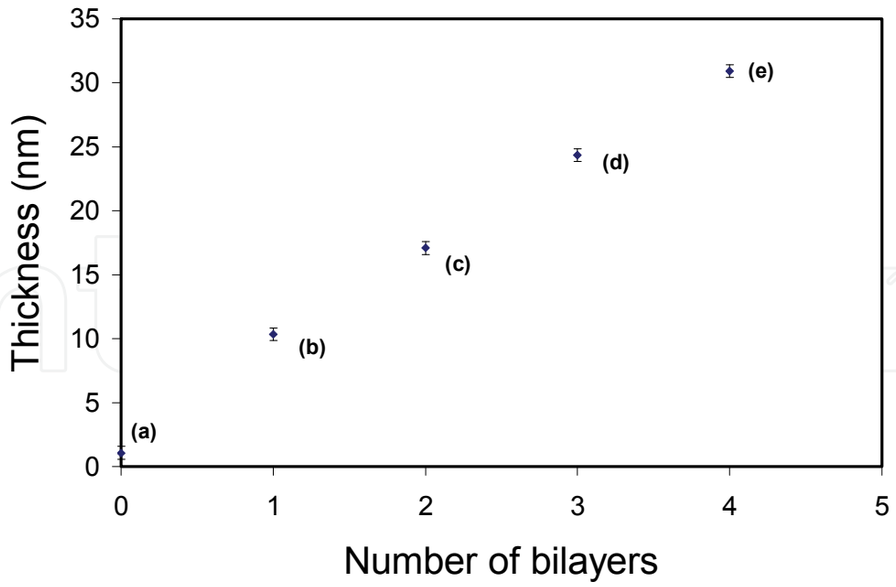

Fig. 2. Ellipsometric thicknesses after the successive addition of following layers: thioctic acid (point a), PLL-Tyr first bilayer (point b), PLL-Tyr second bilayer (point c), PLL-Tyr third bilayer (point d), and PLL and NEST final bilayer (point e). Reproduced with permission from (Kohli et al., 2007).

PLL and Tyr bilayer was approximately 9.3 ± 0.4 nm. The thickness increase for the next two PLL-Tyr bilayers was approximately the same and equal to 7.2± 0.3 nm. The thickness increase following the addition of final PLL-NEST bilayer was approximately 6.6 ± 0.3 nm.

3.2 Dependence of current response on working potential and pH

The various experimental parameters (such as pH and applied potential), which can affect the amperometric determination of phenyl valerate, were optimized. The effect of applied potential on the amperometric response of the sensor was tested in the range between 0.05

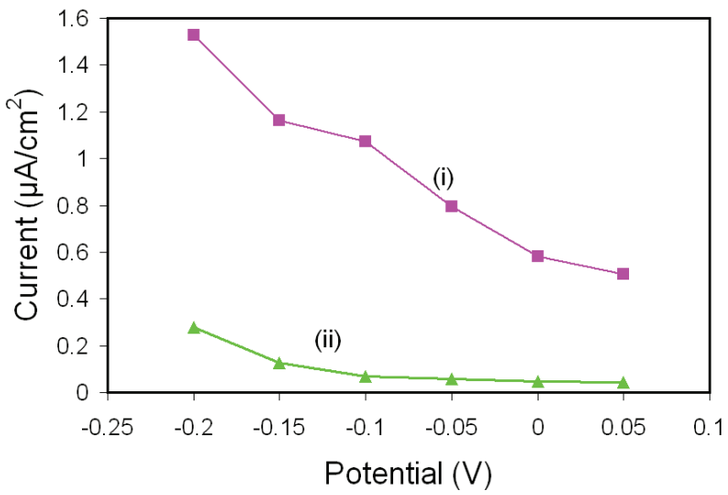

(a)

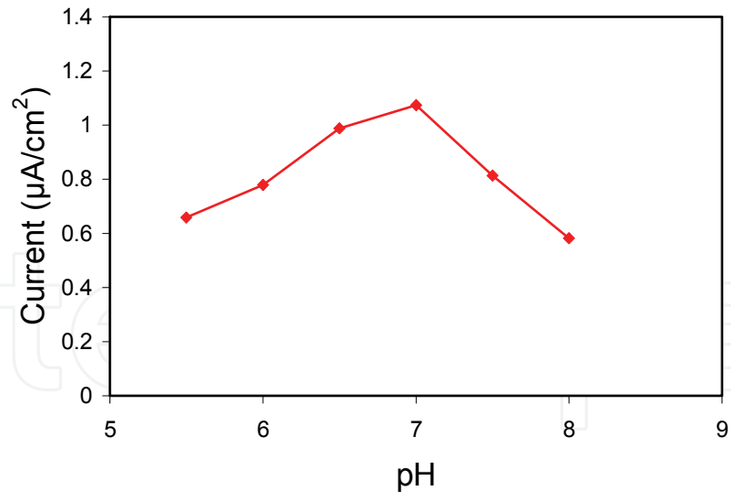

(b)

Fig. 3. (a) Effect of working potential on the response current of the enzyme electrode in 0.1 M phosphate buffer (pH 7.0) with (i) and without (ii) 12 μM phenyl valerate solution, in 0.1 M phosphate buffer at an applied potential of -0.1 V (vs Ag/AgCl). (b) Effect of pH on the response current of the electrode, in the presence of 12 μM phenyl valerate solution, in 0.1 M phosphate buffer at an applied potential of -0.1V (vs Ag/AgCl). Rreproduced with permission from (Kohli et al., 2007).

and -0.20 V. Figure 3a illustrates the signal and background for the whole range. The highest signal-to background ratio, was obtained at -0.1 V. At a working potential more negative than -0.1 V, higher signals were obtained, but the background current also increased distinctly. Therefore, a working potential of -0.1 V was used for further studies. The effect of pH was also studied in the pH range 5.5 to 8.0 in 0.1 M phosphate buffer at working potential of -0.1 V. As shown in Figure 3b, the response current attained a maximum value at pH 7.0. This pH was used for further studies.

3.3 Measurement of esterase activity using NEST biosensor

Figure 4a displays a typical current-time response under the optimal experimental conditions after the successive addition of aliquots of 4 µM phenyl valerate to the phosphate

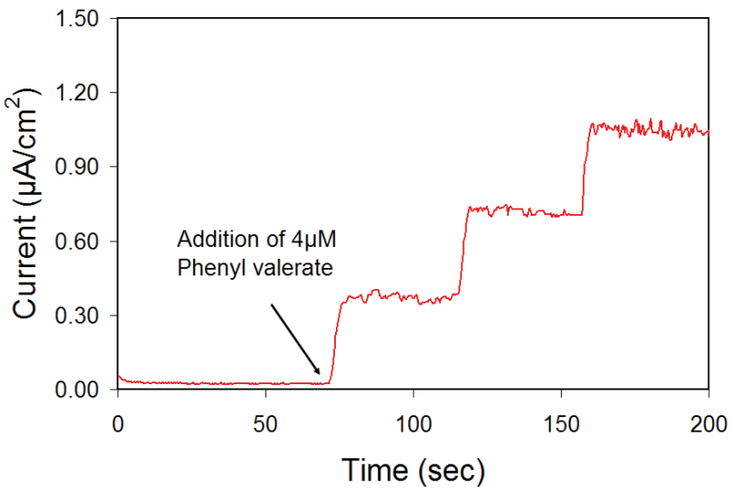

(a)

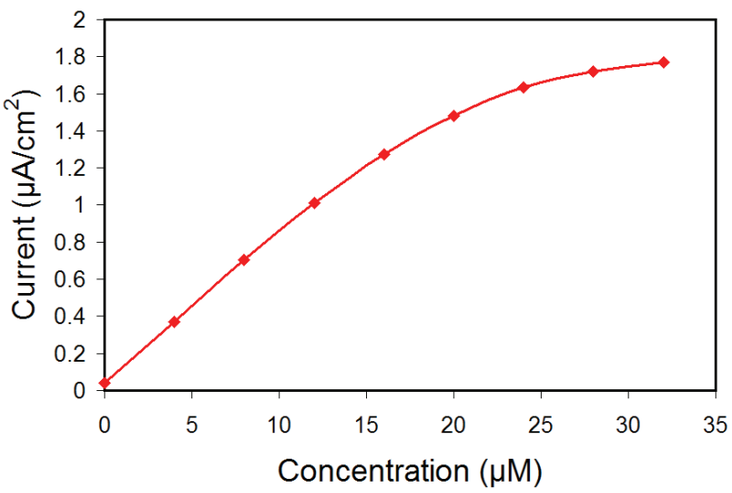

(b)

Fig. 4. (a) Current time response of the NEST biosensor to the addition of aliquots of 4 µM phenyl valerate, in 0.1 M phosphate buffer, pH 7.0, at an applied potential of -0.1V (vs Ag/AgCl). (b) Calibration plot. Reproduced with permission from (Kohli et al., 2007).

buffer. A well defined reduction current, proportional to the amount of phenyl valerate, was observed. The response time of the electrode was less then 20 seconds, due to the nano-scale thickness of the interface. The response to phenyl valerate was linear (r=0.991) in the range 0.5 µM to 12 µM, and it reached saturation at approx. 30 µM (Figure 4b). The limit of detection was 0.5 µM at a signal-to-noise ratio of 3. The reproducibility of the sensor was investigated at a phenyl valerate concentration of 4 µM; the mean current was approximately 348 nAcm-2, with a relative standard deviation of 9.9%. Figure 5 shows a control experiment which was done on an electrode containing only poly-L-lysine and tyrosinase bilayers. As expected, a relatively very small rise in steady state current was observed on the addition of phenyl valerate. The small rise can be attributed to the presence of a small amount of phenol produced due to auto-hydrolysis of phenyl valerate solution.

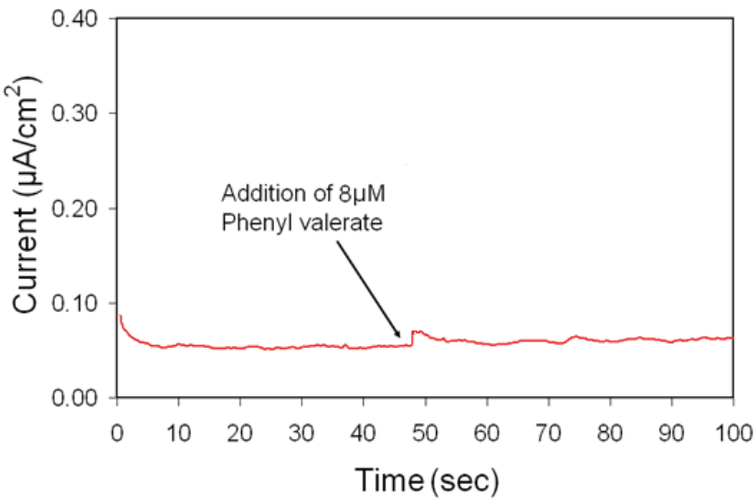

Fig. 5. Control experiment: Current time response on an electrode containing only tyrosinase. The electrode was assembled in exactly the same way as NEST biosensor, except that the final NEST layer was not deposited. The Reproduced with permission from (Kohli et al., 2007).

3.4 Inhibition of esterase activity

To measure inhibition of the esterase activity, an aliquot of phenyl valerate was added to the phosphate buffer. After a steady biosensor signal was obtained, a known quantity of phenylmethylsulfonyl fluoride (PMSF), a non-neuropathic compound previously shown to inhibit NEST (or NTE) esterase activity, was added to the phosphate buffer solution, and the resulting drop in current was measured. At very low concentration there was not an appreciable drop in signal as shown in Figure 6. As shown in Figure 7, however, a 20% (± 3%) decrease in response on the addition of 100 µM PMSF and a 70% (± 4%) decrease on the addition of 1000 µM PMSF was observed as shown in Figure 8. PMSF inhibition of NEST esterase activity reduces the amount of phenol and subsequently *o*-quinone produced. Therefore, less *o*-quinone gets reduced at the electrode surface, leading to a drop in current. These results suggest that the NEST biosensor can be used for concentration-dependent detection of NEST inhibitors.

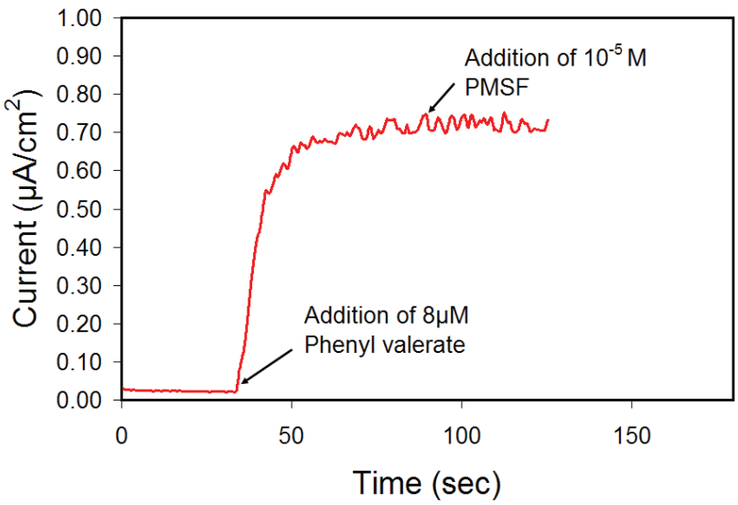

Fig. 6. Current time response of NEST biosensor to the addition of phenyl valerate in phosphate buffer (0.1 M, pH 7.0) to obtain a final phenyl valerate concentration of 8 μM followed by the addition of NEST inhibitor PMSF to obtain a final PMSF concentration of 10 μM. Reproduced with permission from (Kohli et al., 2007).

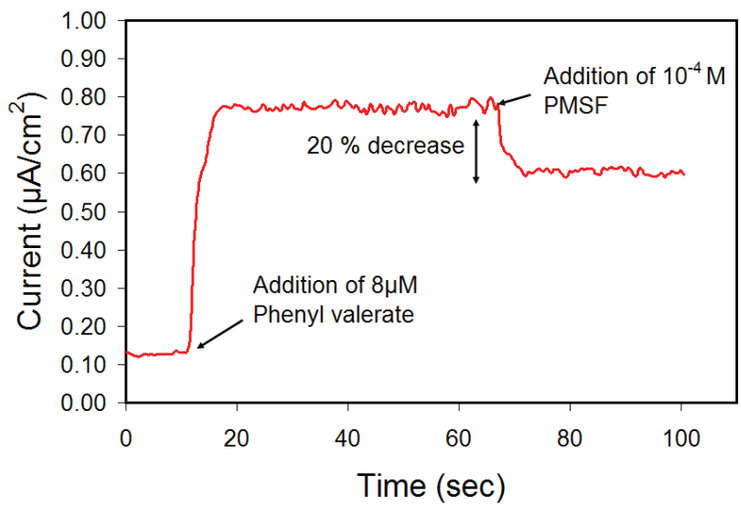

Fig. 7. Current time response of NEST biosensor to the addition of phenyl valerate in phosphate buffer (0.1 M, pH 7.0) to obtain a final phenyl valerate concentration of 8 μM followed by the addition of NEST inhibitor PMSF to obtain a final PMSF concentration of 100 μM. Reproduced with permission from (Kohli et al., 2007).

3.5 Higher-sensitivity NEST biosensor

NEST biosensor sensitivity could be increased by increasing the number of bilayers of PLL-Tyr to six. As discussed by Kohli et. al (Kohli et al., 2007) in the mathematical model developed for the NEST biosensor, the sensitivity can be improved more efficiently by increasing the amount of tyrosinase immobilized on the surface rather than increasing the

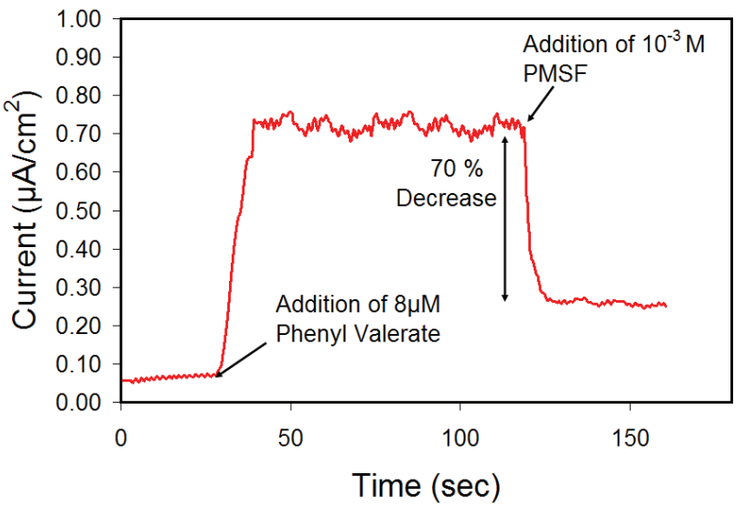

Fig. 8. Current versus time response of the NEST biosensor to the addition of phenyl valerate in phosphate buffer (0.1 M , pH 7.0) to obtain a final phenyl valerate concentration of 8 µM followed by the addition of the NEST inhibitor PMSF to obtain a final PMSF concentration of 1000 µM. Reproduced with permission from (Kohli et al., 2007).

amount of NEST. Hence, we developed a higher-sensitivity sensor by increasing the bilayers to six as the sensitivity of the catechol sensor was maximized with 6 bilayers (Srivastava, 2008). The same procedure used previously for the NEST biosensor was followed to fabricate the higher-sensitivity biosensor. The gold electrode was first modified with thioctic acid followed by the deposition of PLL-Tyr bilayers. After addition of 6 bilayers a layer of NEST was added. The sensor was tested for NEST activity by phenyl valerate assay. The sensitivity went up to 847 ± 158 nA cm-2µM-1 for the addition of phenyl valerate. The plot for phenyl valerate is shown in Figure 9. NEST inhibition was also done by addition of 100 µM and 1mM of PMSF. The decrease in current was the same as observed with 3 bilayers of NEST. The plots for inhibition of NEST on 6 bilayers of PLL-Tyr are shown in Figures 10 and 11 for PMSF concentrations of 100 µM and 1 mM, respectively. There was no remarkable decrease in current with 10 µM addition of PMSF (data not shown). Hence, a higher-sensitivity NEST biosensor can be obtained by increasing the amount of tyrosinase on the interface. It also implies that better sensors can be prepared with marginal increment to cost as tyrosinase is commercially available and can be easily deposited onto the electrode by using LBL deposition.

3.6 Significance of NEST biosensor

This new biosensor approach to measuring NEST esterase activity and its inhibition can in principle easily be extended to full length NTE. The approach offers several advantages over the old two step method. First, it requires only a single step to measure NEST (or NTE) esterase activity. Because the NEST esterase activity is co-immobilized with tyrosinase on the sensor interface, the presence of phenyl valerate triggers sequential reactions that result in an electrical signal. Second, the nanometer-scale thickness of layers in the sensing interface provides a very short diffusion path giving a rapid response time (less than 10 seconds). Third, the biosensor is suitable for continuous, real-time measurements of esterase

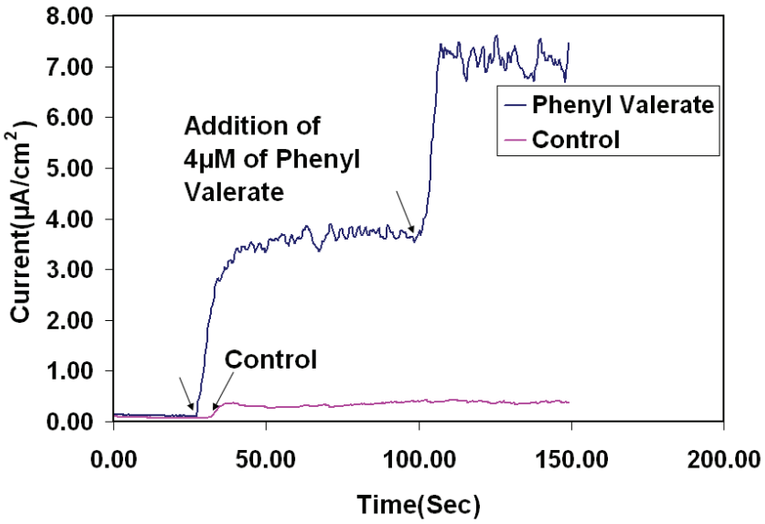

Fig. 9. Current versus time response of the higher-sensitivity NEST biosensor with 6 bilayers of PLL-Tyr underneath the NEST layer. The sensor was tested in phosphate buffer (0.1M) with electrode maintained -0.1V vs Ag/AgCl reference electrode. For the control the electrode was prepared in exactly the same manner but the NEST layer was not added. Reproduced with permission from (Srivastava, 2008).

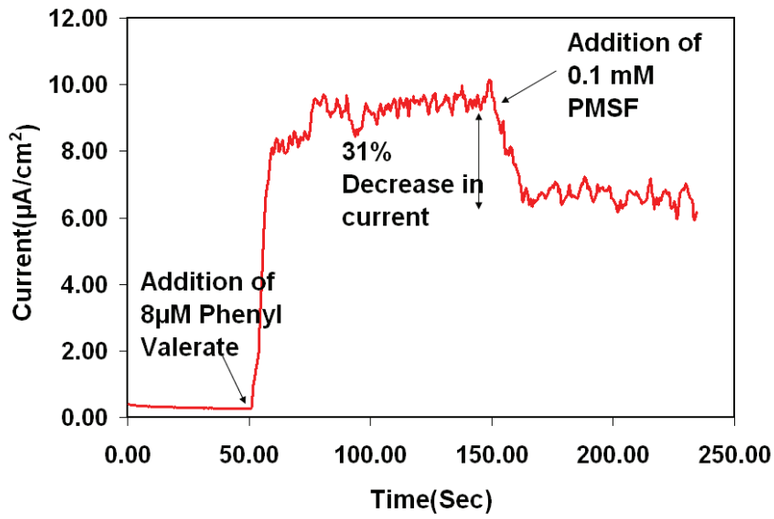

Fig. 10. Current response of the higher-sensitivity NEST biosensor with 6 layers of PLL-Tyr followed by inhibition of NEST by addition of 0.1 mM PMSF. First phenyl valerate was added to get the final substrate concentration of 8 μM in bulk solution. The current response was allowed to achieve steady state before addition of an aliquot of PMSF to get a final inhibitor concentration of 0.1 mM. Reproduced with permission from (Srivastava, 2008).

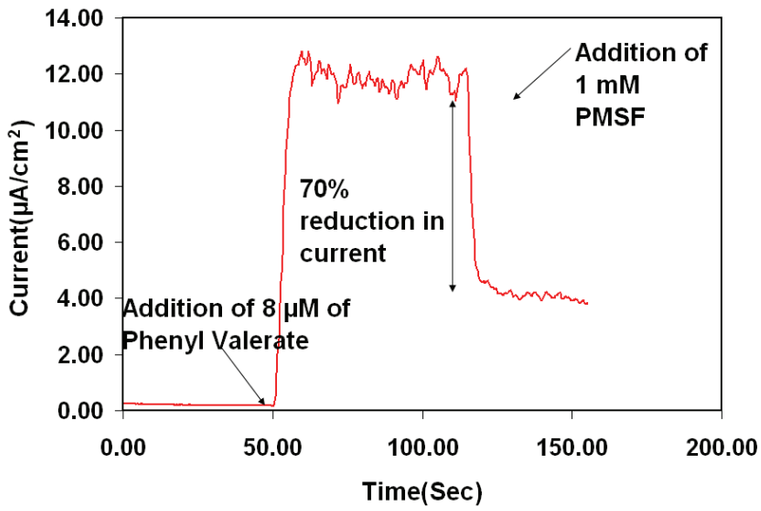

Fig. 11. Current response of the higher-sensitivity NEST biosensor with 6 layers of PLL-Tyr and followed by inhibition of NEST by addition of 1 mM PMSF. First phenyl valerate was added to get the final substrate concentration of 8 μM in bulk solution. The current response was allowed to achieve steady state before addition of an aliquot of PMSF to get a final inhibitor concentration of 1 mM. Reproduced with permission from (Srivastava, 2008).

activity. Fourth, the biosensor is designed to achieve signal amplification via recycling of *o*-quinone to catechol, thus increasing the sensitivity of the sensor. Fifth, the biosensor interface is generated by flexible, layer-by-layer (LBL), molecular self-assembly methods that would allow it to be assembled on electrodes inside microfluidic channels, thus enabling the production of high-density biosensor arrays consisting of various esterases (e.g., AchE and BchE) for high-throughput applications.

This combination of desirable properties makes this interface well suited for important applications, including studying the kinetic properties of esterases such as NEST protein, high-throughput screening of compounds for NEST (or NTE) inhibition and continuous, on-line, environmental monitoring to detect chemical warfare agents that target NEST (or NTE) and other esterases.

4. Conclusions

A biosensor has been developed that allows the activity of NEST to be measured continuously. The biosensor was fabricated by a layer-by-layer assembly approach to co-immobilize NEST and tyrosinase on a gold electrode. Ellipsometry provided evidence for the sequential assembly of the multiple layers that make up the interface. Constant potential voltammetry allowed NEST enzyme activity to be measured with a rapid response time (< 10 s). The biosensor gave a concentration-dependent response to a known non-neuropathic (PMSF) NEST inhibitor.

5. Acknowledgment

This work was funded in part by the National Science Foundation (0609164, 0756703, and 0832730), the U.S. Army Research Office (DAAD19-02-1-0388), the University Research Corridor, and the MSU Foundation.

6. References

Atkins, J. & Glynn, P. (2000). Membrane association of and critical residues in the catalytic domain of human neuropathy target esterase. *Journal of Biological Chemistry* 275, 32, 24477-24483.

Coche-Guerente, L.; Labbe, P. & Mengeaud, V. (2001). Amplification of amperometric biosensor responses by electrochemical substrate recycling. 3. Theoretical and experimental study of the phenol-polyphenol oxidase system immobilized in Laponite hydrogels and layer-by-layer self-assembled structures. *Analytical Chemistry* 73, 14, 3206-3218.

Decher, G. (1997). Fuzzy nanoassemblies: Toward layered polymeric multicomposites. *Science* 277, 5330, 1232-1237.

Forshaw, P. J.; Atkins, J.; Ray, D. E. & Glynn, P. (2001). The catalytic domain of human neuropathy target esterase mediates an organophosphate-sensitive ionic conductance across liposome membranes. *Journal of Neurochemistry* 79, 2, 400-406.

Forzani, E. S.; Solis, V. M. & Calvo, E. J. (2000). Electrochemical behavior of polyphenol oxidase immobilized in self-assembled structures layer by layer with cationic polyallylamine. *Analytical Chemistry* 72, 21, 5300-5307.

Glynn, P. (1999). Neuropathy target esterase. *Biochemical Journal* 344, 625-631.

Kayyali, U. S.; Moore, T. B.; Randall, J. C. & Richardson, R. J. (1991). Neurotoxic Esterase (Nte) Assay - Optimized Conditions Based on Detergent-Induced Shifts in the Phenol/4-Aminoantipyrine Chromophore Spectrum. *Journal of Analytical Toxicology* 15, 2, 86-89.

Kohli, N.; Hassler, B. L.; Parthasarathy, L.; Richardson, R. J.; Ofoli, R. Y.; Worden, R. M. & Lee, I. (2006). Tethered lipid bilayers on electrolessly deposited gold for bioelectronic applications. *Biomacromolecules* 7, 12, 3327-3335.

Kohli, N.; Srivastava, D.; Sun, J.; Richardson, R. J.; Lee, I. & Worden, R. M. (2007). Nanostructured biosensor for measuring neuropathy target esterase activity. *Analytical Chemistry* 79, 14, 5196-5203.

Kropp, T. J.; Glynn, P. & Richardson, R. J. (2004). The mipafox-inhibited catalytic domain of human neuropathy target esterase ages by reversible proton loss. *Biochemistry* 43, 12, 3716-3722.

Li, Y.; Dinsdale, D. & Glynn, P. (2003). Protein domains, catalytic activity, and subcellular distribution of neuropathy target esterase in mammalian cells. *Journal of Biological Chemistry* 278, 10, 8820-8825.

Makhaeva, G. F.; Sigolaeva, L. V.; Zhuravleva, L. V.; Eremenko, A. V.; Kurochkin, I. N.; Malygin, V. V. & Richardson, R. J. (2003). Biosensor detection of neuropathy target esterase in whole blood as a biomarker of exposure to neuropathic organophosphorus compounds. *Journal of Toxicology and Environmental Health-Part A* 66, 7, 599-610.

Rainier, S.; Bui, M.; Mark, E.; Thornas, D.; Tokarz, D.; Ming, L.; Delaney, C.; Richardson, R. J.; Albers, J. W.; Matsunami, N.; Stevens, J.; Coon, H.; Leppert, M. & Fink, J. K. (2008). Neuropathy target esterase gene mutations cause motor neuron disease. *American Journal of Human Genetics* 82, 3, 780-785.

Richardson, R. J.; Worden, R. M. & Makhaeva, G. F. (2009). Biomarkers and biosensors of delayed neuropathic agents. *Handbook of Toxicology of Chemical Warfare Agents* R. C. Gupta. Amsterdam, Academic Press/Elsevier**:** 859-876.

Sigolaeva, L. V.; Makower, A.; Eremenko, A. V.; Makhaeva, G. F.; Malygin, V. V.; Kurochkin, I. N. & Scheller, F. W. (2001). Bioelectrochemical analysis of neuropathy target esterase activity in blood. *Analytical Biochemistry* 290, 1, 1-9.

Sokolovskaya, L. G.; Sigolaeva, L. V.; Eremenko, A. V.; Gachok, I. V.; Makhaeva, G. F.; Strakhova, N. N.; Malygin, V. V.; Richardson, R. J. & Kurochkin, I. N. (2005). Improved electrochemical analysis of neuropathy target esterase activity by a tyrosinase carbon paste electrode modified by 1-methoxyphenazine methosulfate. *Biotechnology Letters* 27, 16, 1211-1218.

Srivastava, D. (2008). Fabrication of nanostructures and nanostructure based interfaces for biosensor application. *PhD Dissertation*, Michigan State University, East Lansing, MI.

van Tienhoven, M.; Atkins, J.; Li, Y. & Glynn, P. (2002). Human neuropathy target esterase catalyzes hydrolysis of membrane lipids. *Journal of Biological Chemistry* 277, 23, 20942-20948.

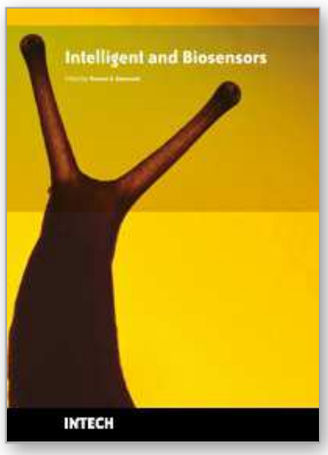

Intelligent and Biosensors

Edited by Vernon S. Somerset

ISBN 978-953-7619-58-9
Hard cover, 386 pages
Publisher InTech
Published online 01, January, 2010
Published in print edition January, 2010

The use of intelligent sensors have revolutionized the way in which we gather data from the world around us, how we extract useful information from that data, and the manner in which we use the newly obtained information for various operations and decision making. This book is an attempt to highlight the current research in the field of Intelligent and Biosensors, thereby describing state-of-the-art techniques in the field and emerging new technologies, also showcasing some examples and applications.

How to reference

In order to correctly reference this scholarly work, feel free to copy and paste the following:

Devesh Srivastava, Neeraj Kohli, Rudy J. Richardson, Robert M. Worden, and Ilsoon Lee (2010). Neuropathy Target Esterase Biosensor, Intelligent and Biosensors, Vernon S. Somerset (Ed.), ISBN: 978-953-7619-58-9, InTech, Available from: http://www.intechopen.com/books/intelligent-and-biosensors/neuropathy-target-esterase-biosensor

INTECH
open science | open minds

InTech Europe
University Campus STeP Ri
Slavka Krautzeka 83/A
51000 Rijeka, Croatia
Phone: +385 (51) 770 447
Fax: +385 (51) 686 166
www.intechopen.com

InTech China
Unit 405, Office Block, Hotel Equatorial Shanghai
No.65, Yan An Road (West), Shanghai, 200040, China
中国上海市延安西路65号上海国际贵都大饭店办公楼405单元
Phone: +86-21-62489820
Fax: +86-21-62489821

IntechOpen